

**A new system for real-time data acquisition and pulse parameterization  
for digital positron annihilation lifetime spectrometers with high  
repetition rates**

Hirschmann, E.; Butterling, M.; Hernandez Acosta, U.; Liedke, M. O.; Elsherif, A. G. A.;  
Petring, P.; Görlner, M.; Krause-Rehberg, R.; Wagner, A.;

Originally published:

August 2021

**Journal of Instrumentation 16(2021), 8001-8017**

DOI: <https://doi.org/10.1088/1748-0221/16/08/P08001>

Perma-Link to Publication Repository of HZDR:

<https://www.hzdr.de/publications/Publ-32979>

Release of the secondary publication  
on the basis of the German Copyright Law § 38 Section 4.

# **A new system for real-time data acquisition and pulse parameterization for digital Positron Annihilation Lifetime Spectrometers with high repetition rates**

---

**E. Hirschmann <sup>a,1</sup>, M. Butterling <sup>a</sup>, U. Hernandez Acosta <sup>a,b</sup>, M. O. Liedke <sup>a</sup>,  
A. G. Attallah <sup>a</sup>, P. Petring <sup>a</sup>, M. Görler <sup>a</sup>, R. Krause-Rehberg <sup>c</sup>, and A. Wagner <sup>a</sup>**

<sup>a</sup>*Helmholtz-Zentrum Dresden-Rossendorf, Institute of Radiation Physics  
Bautzner Landstr. 400, 01328 Dresden, Germany*

<sup>b</sup>*Helmholtz-Zentrum Dresden-Rossendorf, Center for Advanced Systems Understanding  
Am Untermarkt 20, 02826 Görlitz, Germany*

<sup>c</sup>*Martin Luther University Halle-Wittenberg, Department of Physics  
Von-Danckelmann-Platz 3, 06120 Halle, Germany*

*E-mail: e.hirschmann@hzdr.de*

**ABSTRACT:** We present a new system for high repetition rate and real-time pulse analysis implemented at the Monoenergetic Positron Source (MePS) at the superconducting electron LINAC ELBE at Helmholtz-Zentrum Dresden-Rossendorf. Dedicated digital signal processing and optimized algorithms are employed allowing for high bandwidth throughput, online pulse analysis and filtering. Positrons generated from radioisotopes and from bremsstrahlung pair production by means of highly intense accelerator-based positron beams serve as a microstructure probe allowing material characterizations with respect to chemical, mechanical, electrical, and magnetic properties. Positron annihilation lifetime events with up to 13 MHz repetition rate are being processed online without losses while performing signal selections for pile-up reduction, online energy calibration, and – for radioisotope-based measurements – identification of start and stop events.

**KEYWORDS:** Data acquisition concepts; Digital signal processing (DSP); Online farms and online filtering; Data processing methods; Data reduction methods; Detection of defects;

---

<sup>1</sup> Corresponding author.

## Contents

<b>1. Introduction</b>	<b>2</b>
1.1. Positron Annihilation Spectroscopy	2
1.2. Beam-based PALS	3
<b>2. Digital data acquisition and online pulse analysis</b>	<b>3</b>
2.1. General information on digitization	3
2.2. Introduction into MePS	4
2.3. High performance PALS	6
2.3.1. 1 <sup>st</sup> Level: Data collection	6
2.3.2. 2 <sup>nd</sup> Level: Data processing	7
2.3.3. 3 <sup>rd</sup> Level: Data allocation and parallelization	9
2.4. Performance tests	10
2.5. Super-Singles Filter	11
2.6. Automated energy calibration	12
<b>3. Summary</b>	<b>13</b>
<b>4. References</b>	<b>14</b>

## 1. Introduction

### 1.1. Positron Annihilation Spectroscopy

Positron annihilation spectroscopy (PAS) is a highly sensitive method for characterizing atomic imperfections, such as lattice defects or dislocations [1]. Furthermore, with the help of the hydrogen-like bound state of positron and electron, called positronium, PAS allows determining the sizes of open and closed micro- and mesopores (0.3 - 100 nm) via the positron lifetime decay [2]. The fate of a positron embodies generation, implantation into matter, thermalization, diffusion, formation of positronium (if possible) and finally annihilation. Positrons are commonly generated either by  $\beta^+$  decays of radioactive isotopes such as  $^{22}\text{Na}$  or by pair production by energetic x-rays from electron bremsstrahlung or  $\gamma$ -rays from neutron-capture reactions in fission reactors. Following their generation, positrons are implanted into the material under study with various energies, where they approach thermal equilibrium with the sample body through inelastic collisions, various excitation mechanisms or scattering by phonons [3]. Subsequently, positrons diffuse inside the crystal lattice in a 3-dimensional random-walk process until annihilating with an electron by emitting two characteristic 511 keV photons [4] or they form positronium with an electron from the thermalization track [5], and finally annihilating through two or three gamma quanta depending on the relative spin orientation [6]. Detection of these released gamma quanta forms the basis of positron experiments and reflects material characteristics due to their angular, energy or annihilation lifetime distribution.

## **1.2. Beam-based PALS**

The investigation of defect concentration, defect type, pore size or pore size distribution are main topics of positron annihilation lifetime spectroscopy (PALS), where the time difference of generation and annihilation provides information about the electron density at the annihilation site or the free volume. Particularly, investigations of thin films or multi-layered systems become increasingly relevant for fundamental science and industrial applications. Dedicated instruments that are capable of investigating not only the surface or a small section of the sample at atomic levels are in high demand. Mono-energetic positron beams with energies from a few dozens of eV up to 20 keV allow investigating depth profiles of defects or pores from the surface to depths of sub-micrometer.

Intense positron beams, which yield quite high intensities, are found at nuclear research reactors or at electron accelerators. See for example: NEPOMUC at the research reactor in Munich (Germany) [7], [8], POSH at the research reactor Delft (the Netherlands) [9], TIPS research reactor in Austin (Texas) [10], PULSTAR in Raleigh (North Carolina) [11] or KUR in Kyoto (Japan) [12] as well as accelerator based beam lines like: the positron beam at Lawrence Livermore National Laboratory (California) [13], the micro-beam at National Institute of Advanced Industrial Science and Technology (AIST) in Tsukuba (Japan) [14], the positron beam facility at the High Energy Accelerator Research Organization (KEK) in Tsukuba (Japan) [15] and, last but not least, the monoenergetic positron source (MePS) at Helmholtz-Zentrum Dresden-Rossendorf (Germany) [16].

## **2. Digital data acquisition and online pulse analysis**

This section presents the progress and advantages of a fully digital signal processing on the positron beam-based MePS system. Although a large part of the problems could be met by choosing C++ as a high-level programming language and Qt as a platform for graphical user interfaces, the performance of the system was strongly related to the algorithm. We plan to make the next version of the source code available in a mature version via an open source platform. This has not yet been done for the current version. In the following, we show how technical and software adaptations are used to speed up the processing and improve the quality of the positron lifetime spectra.

### **2.1. General information on digitization**

Digitization in the context of PALS refers to the transformation of a continuous signal, e.g., anode voltage of a photo-multiplier tube coupled to a scintillating crystal, into time-discrete values by employing high-speed analogue-to-digital convertors.

The development of digital systems for recording positron annihilation lifetime spectra started in early 2000er. Groups in Japan [17], [18] and Finland [19], [20] recorded the first fully-digital lifetime spectra based on fast digital oscilloscopes. In the following years, many other laboratories [21]–[26] performed a transition from analogue to digital technology. The advantages of digital data acquisition became increasingly visible. The improved quality and time resolution of the lifetime spectra [27], the simple

installation of a station, the free choice of time windows or channel dispersions, the use of filter algorithms [28], the increased long-term and temperature stability [29], as well as the high functionality and flexibility are still reasons for more and more groups to upgrade their systems. In digital systems, especially once digitized pulse becomes immune to distortion, electronic noise or other operational fluctuations [30]. In addition, the raw data of the detector can be archived for offline analysis, giving the user better control over analysis parameters [30]. Thus, systematic studies based on list mode data can help to evaluate parameters without interference from repeated measurements.

However, in most cases the conversion from analogue to digital data processing took place at source-based and not beam-based systems. The reason for the delayed implementation in beam-based systems is primarily given by the increasingly large amount of data traffic due to the higher event rates at reactor- or accelerator-driven systems. High-resolution and high-speed digitizers generate larger data packages, which have to be transmitted to the analysis computer and have to be handled fast enough in order to perform an online analysis or pulse parameterization. This increasingly limits the maximum bandwidth or counting rate of a system, and it demands higher data processing rates than analogue components.

## **2.2. Introduction into MePS**

In order to illustrate the goal of digitization, some key information about MePS, the Mono-energetic Positron Source, are described in the following. The MePS system results from a joint project of Martin Luther University Halle-Wittenberg and Helmholtz Zentrum Dresden-Rossendorf and is one of the user beamlines at the large-scale research facility ELBE Center for High-Power Radiation Sources. A schematic depiction is shown in Figure 1.

Positron generation at MePS based on pair production caused by a pulsed, superconducting electron accelerator called ELBE [31], Figure 1 (a). Bunches of electrons with an energy of about 35 MeV impinge through a beryllium window Figure 1 (b) onto a water-cooled tungsten converter creating bremsstrahlung, Figure 1 (c). The high-intensity bremsstrahlung in turn generates electron-positron pairs in a tungsten foil located behind the converter, enabling positrons to emerge from the tungsten surface with a defined energy of 3 eV [32] in a process called moderation [33]. Subsequently, the moderated positrons are accelerated by a DC electric field to a transport energy of 2 keV and focused into a magnetic guiding field via an electrostatic lens Figure 1 (e) and transported towards the sample chamber, Figure 1 (k).

Consequently, a pulsed electron beam generates a pulsed positron beam. While the electron beam has about 10 ps pulse width, the energy dispersion of the positron beam leads to a temporal broadening which is compensated by a chopper and buncher section close to the sample chamber but prior to post-acceleration, Figure 1 (g), (h) and (i).

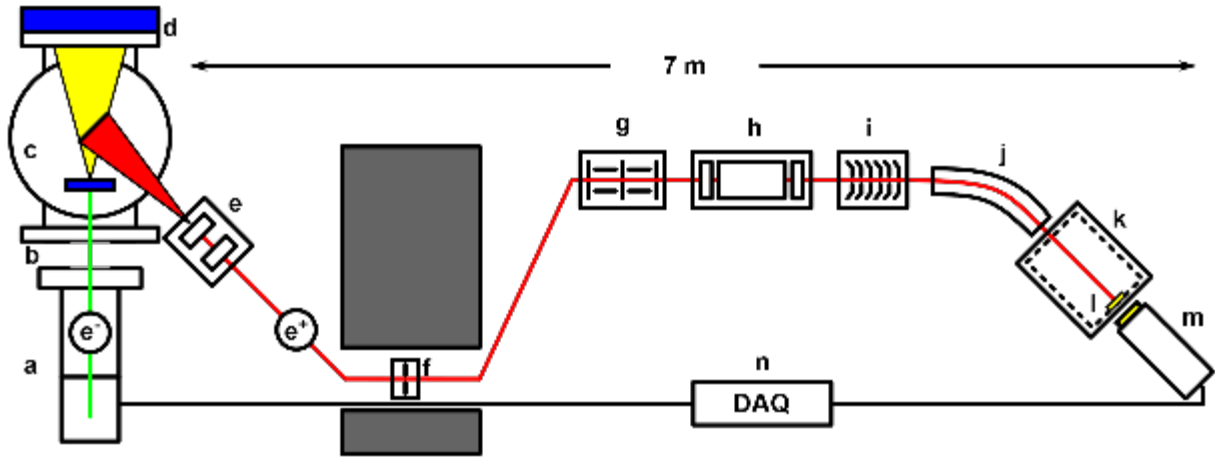


Figure 1: Schematic depiction of the MePS system Systems: (a) electron source ELBE, (b) beryllium window, (c) converter and moderator, (d) aluminum block, (e) extraction lens, (f) aperture wagon, (g) chopper, (h) buncher, (i) accelerator, (j) bent tube, (k) sample chamber with Faraday cage, (l) sample, (m) scintillation detector, (n) digital data acquisition.

The operating frequency of ELBE and thus of MePS can be freely selected with a divider of  $2^n$  of 13 MHz ( $n = 0, \dots, 8$ ). Usually, a repetition rate of 1.625 MHz ( $n = 3$ ) is selected for positron annihilation lifetime experiments in order to avoid pulse overlap for longer annihilation lifetimes. Therefore, it is possible to measure relatively short positron lifetimes e.g., carbon with 393 ps, and relatively long positron lifetimes e.g., micro or mesoporous films with 5 to 100 ns, within the same setup at different implantations energies in 60 s per energy [34].

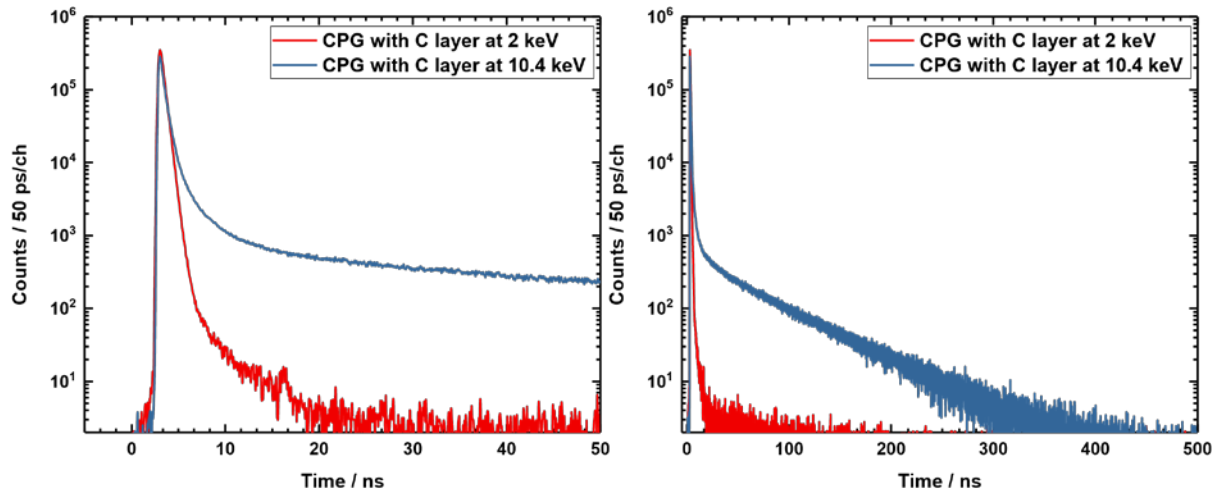


Figure 2: Positron annihilation lifetime spectrum for controlled porous glass (CPG) with 280 nm carbon layer on top, measured at 2 keV (red) and 10.4 keV (blue) positron implantation energy at MePS.

The RF signal serves as the time-start for determining the positron lifetime. The time stop is defined by detecting the annihilation radiation, which is registered by a  $\text{CeBr}_3$  scintillator (2.54 cm thickness; 5.08 cm diameter) coupled to a Hamamatsu R13089 photomultiplier tube (PMT) located behind the sample chamber. Due to the large detector efficiency and the high number of impinging positrons, count rates

of about 170 kcps at 1.62 MHz are reached. The time difference between RF timing signal and annihilation measures the positron lifetime shifted by a constant transport time. The main challenge of digitization was to implement an online data processing that is able to detect the pulses of the PMT, distinguish signal from background, assign them to the appropriate RF timing signal, calculate the time difference and display the time difference histogram i.e., positron annihilation lifetime spectrum.

### 2.3. High performance PALS

To address these challenges, we use three levels of digitization. The first level is a digitizer with FPGA-based trigger logic that allows channels to be triggered individually while it uses only a small time region around the pulse to be recorded and transmitted to the analysis computer. The second level is a sophisticated processing algorithm that minimizes the calculation time of the pulse maximum and timestamp without compromising precision. The third and final level is a parallelized calculation that exploits the full potential of the processor by implementing a waterfall-like data processing on multiple cores.

#### 2.3.1. 1<sup>st</sup> Level: Data collection

At the beginning of the electronic data processing, an analogue-to-digital converter converts the continuous-time and continuous-amplitude signal from the detector – here a photomultiplier tube connected to a CeBr3 scintillator – to a discrete-time and discrete-amplitude digital signal with a given bit depth. In conventional digital systems, a fixed time window is recorded with respect to a trigger and transmitted to the analysis computer. Consequently, large amounts of data are being transferred for further analysis when large time windows have to be covered, as it is the case for long annihilation lifetimes. As an example, a digitizer with 2 GS/s sample rate transmits 1300 data points per event per channel for a time window of 650 ns, see Figure 3. Given a common PMT signal spanning of about 20 ns implies that 97% of the recorded data points contain no information about the signal. Furthermore, it is up to the quality of the trigger, how many signals or whether a signal at all is recorded.

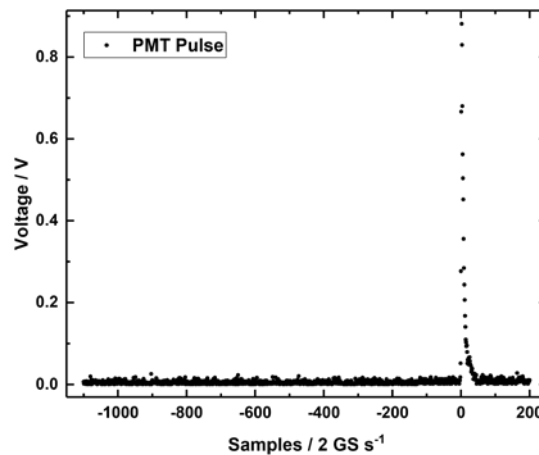


Figure 3: Inverted PMT signal for 2 GS/s sample rate and a 650 ns long time window.

Taking the sample rate of 2 GS/s, a digitizer resolution between 9 and 16 Bit, and two channels (time reference and detector signal) results in a sustained data transfer rate of about 7.5 GB/s, which can barely be handled in an economically feasible way.

In order to reduce the data traffic, we employed the *Teledyne SPDevices ADQ14-DC-2X-MTCA* digitizer with 2 GS/s, 14 bit and pulse detection performed on an integrated FPGA. The firmware enables the transmitted points to be reduced to a predefined range around the pulse (20 ns, 40 points), see Figure 4 left. In addition, the input channels of the digitizer running independently with each detected pulse getting an individual rough timestamp of the internal FPGA clock. Consequently, only essential data for further data processing are transmitted. The 1<sup>st</sup> level data collection decreases the data traffic by a factor of 20.

### **2.3.2. 2<sup>nd</sup> Level: Data processing**

The information that needs to be determined from the tailored pulse are the amplitude (proportional to the energy deposition in the detector) and the time-of-arrival. The pulse amplitude selection allows identifying start and stop events in conventional radioactive source-based positron annihilation lifetime experiments and filtering against background or scattered events. Furthermore, the amplitude serves a constant fraction timing (CFT) algorithm for accurate determination of the time-of-arrival [35]. Hui et al. [24] showed the effect of different interpolation or fitting algorithms in dependence of the digitizer's sampling rate and the selected CFT level on the timing resolution of a PALS system. However, the disadvantages of those individual approaches are: complex numerical functions and a large temporal width of the pulse in order to adjust the shape or interpret the region between digitization points.

With the aim of developing a powerful and functional algorithm, we abstained from using a full peak interpolation, because tests showed that the improvements in timing resolution with and without a full peak interpolation were negligible. Instead, we used only the pulse maximum and a simplified algorithm for the rising edge. A fourth order polynomial fit in five points was chosen with the central point of the polynomial set next to the calculated CFT level, see Figure 4 right.

$$y[x] = a_0 + a_1x + a_2x^2 + a_3x^3 + a_4x^4 \quad (1)$$



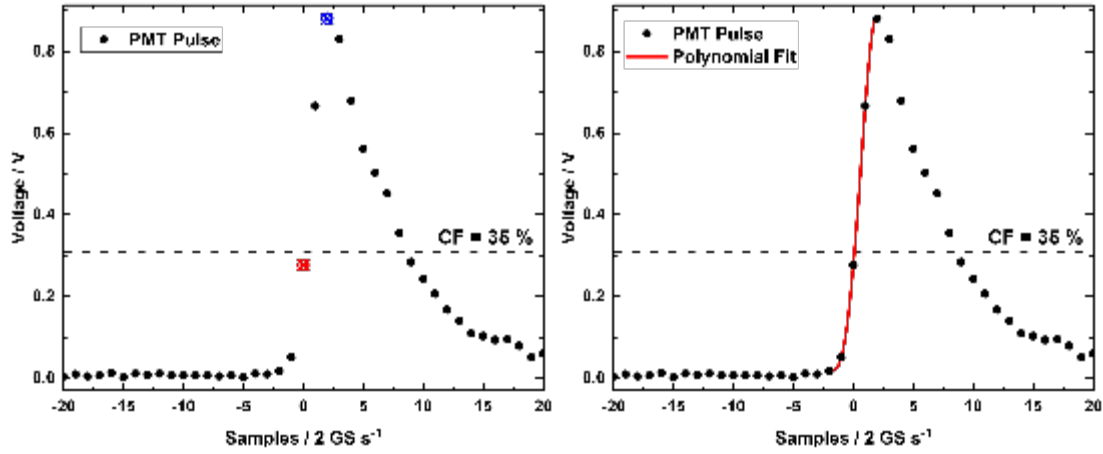


Figure 4: Inverted PMT timing signal for 2 GS/s and 20 ns with pulse maximum (blue dot), central point closest to CF level (red dot), 4th order polynomial fit (red line).

This approach has the advantage, that the required coefficients could be simplified by numerically shifting the time zero point to the CFT intersection point.

Solving the Vandermonde matrix for (1) leads to:

$$\begin{pmatrix} a_0 \\ a_1 \\ a_2 \\ a_3 \\ a_4 \end{pmatrix} = \frac{1}{24t_{SI}^4} \begin{pmatrix} 24t_{SI}^4 y_3 \\ 2t_{SI}^3 (y_1 - 8y_2 + 8y_4 - y_5) \\ -t_{SI}^2 (y_1 - 16y_2 + 30y_3 - 16y_4 + y_5) \\ 2t_{SI} (-y_1 + 2y_2 - 2y_4 + y_5) \\ y_1 - 4y_2 + 6y_3 - 4y_4 + y_5 \end{pmatrix} \quad (2)$$

with  $t_{SI}$  being the sample period. In order to reduce the problem to a root-finding we shift the coordinate system towards the CFT level.

$$a_0^* = a_0 - y_{CFD} \quad (3)$$

To avoid numerically demanding root functions or case selections associated with the analytical solution of a fourth degree polynomial, which also requiring large resources of the processor, we implemented the iterative Householder method [36] for root-finding of scalar real functions.

$$x_{n+1} = x_n + \alpha \frac{\frac{\partial^{\alpha-1}}{\partial x^{\alpha-1}} \left( \frac{1}{f[x_n]} \right)}{\frac{\partial^\alpha}{\partial x^\alpha} \left( \frac{1}{f[x_n]} \right)} \quad (4)$$

Here,  $\alpha$  is the degree of the Householder method (e. g.  $\alpha = 1$  corresponds to the Newton method,  $\alpha = 2$  to the Halley method). With increasing order of the applied polynomial, the convergence rate increases and the accuracy of the numerical solution can already be sufficient for the first iterations. However, this advantage is accompanied by an increasing complexity of the iteration function. Fortunately, this is a negligible problem for our application. On one hand, the solution of the first iteration of the

Householder method has sufficient precision for the application in positron annihilation lifetime spectroscopy, and on the other hand, by shifting the CF point to a virtual time zero point, the first iteration could be carried out with the initial value  $x$  equals 0. Using (4) with  $x_0 = 0$ , the polynomial (1), the coefficients from (2) and (3) we obtain a simplified form:

$$x_1 = \frac{a_0^*(2 a_0^* a_1 a_2 - a_0^{*2} a_3 - a_1^3)}{a_1^4 - 3 a_0^* a_1^2 a_2 + 2 a_0^{*2} a_1 a_3 + a_0^{*2} (a_2^2 - a_0^* a_4)} \quad (5)$$

By that, the numerical root determination reduces to a single term, which only requires simple arithmetic operations. Thus, this approach avoids complex functions such as roots or higher exponents as well as case selections, since the choice of the start value and the form of the polynomial almost guarantees convergence at the searched intersection point. Combining the fine time stamp from the CF timing and the rough time stamp from the FPGA clock, one obtains a global time stamp (6) for each pulse, which can be combined or compared with other pulses, for example to determine the positron annihilation lifetime.

$$t = t_{\text{FPGA}} + x_1 \quad (6)$$

### 2.3.3. 3<sup>rd</sup> Level: Data allocation and parallelization

Once the detector signals being processed and a time stamp being calculated, the independent time stamps of RF and detector have to be correlated in time. To further accelerate the processing and to use the full potential of the processor, three major steps were processed in parallel: data collection, processing and allocation. Since the individual steps depend on each other, a waterfall-like logic was implemented. We employed a buffered data collection in order to efficiently parallelize the data processing.

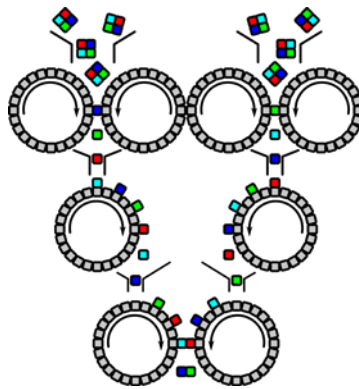


Figure 5: Schematic depiction of the multithreading process for a digitizer with four channels.

## 2.4. Performance tests

In order to quantify the efficiency of the individual optimisation phases, we employed a signal generator with variable frequency as a reference and split it into two input channels. Figure 6 shows the generator frequency and the corresponding processing rate of the respective algorithm. It can be seen that the change from a standard digitizer (*Acqiris DC282*) to an FPGA-based peak detection system (*Teledyne SPDevices ADQ14-DC-2X*) with the same pulse analysis algorithm (cubic spline interpolation), allowed going from 5 kcps to almost 100 kcps.

Further optimisation was obtained through implementation of the aforementioned waterfall-like parallelisation of data processing. Multithreading of the software increased the performance up to 375 kcps. Additionally implementing the Householder root-finding drives the processing rate up to a maximum of 5.6 Mcps per channel.

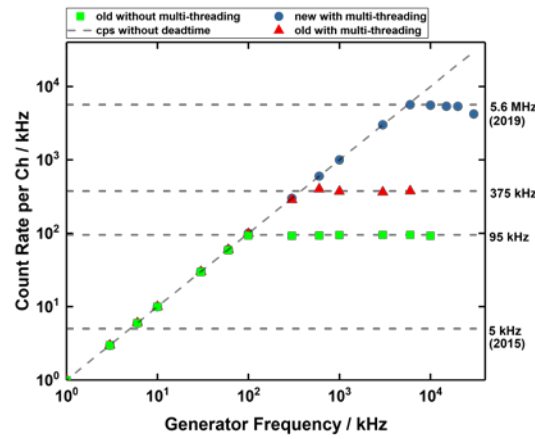


Figure 6: Pulse processing rate per channel as function of the generator frequency: with pulse detection but without multi-threading (green), with pulse detection and with multi-threading (red), with pulse detection, with multi-threading and Householder approach (blue)

In order to test the optimised algorithm and hardware in case of an uncorrelated time signal distribution, one input was coupled to the pulse generator and the second one to a stochastic signal of a radioactive source, see Figure 7. It can be seen that the time differences of the test source can be processed free from dead-time-related dips or a memory overflow; the source count rate of 25 kcps dominates the system rate up to a generator frequency of 13 MHz. Consequently, the hardware and software can be used to determine the occurrence of rare events coupled with respect to a high frequency time reference. Consequently, this System can also be adapted for other systems or experiments as well as for positron annihilation lifetime spectroscopy. An implementation for prompt gamma-ray timing in proton-beam based tumor therapy for in-vivo dose verifications [37] is under way.

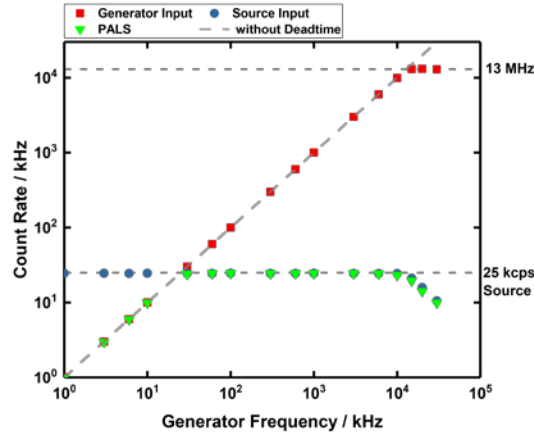


Figure 7: Pulse processing rate for a stochastic signal with 25 kcps and a variable frequency generator. Processing rate source input (PMT) (blue), processing rate generator input (red) and combined processing rate compared to a PALS experiment (green)

## 2.5. Super-Singles Filter

The occurrence of detected or undetected pile-up events, namely the arrival of more than one time signal in a given time window (see Figure 8) has to be prevented in order to avoid a systematic bias. The *super-singles filter* suppresses events in close temporal vicinity.

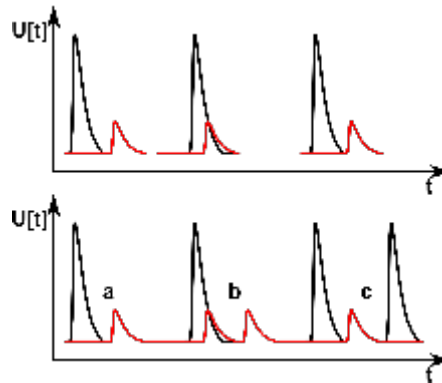


Figure 8: Schematic depiction of a pileup event with a virtual (top) and an actual image (bottom): a) Unique start-stop allocation, b) Stop-stop error, c) Start-start error.

In contrast to conventional trigger logics, this approach not only checks the recorded time window, but also the chronologically preceding and following pulses in the same channel. Thus, excluding the occurrence of other pulses besides the searched start or stop signal, which would falsify an unambiguous assignment and the calculation of the time difference. Tests on source-based PALS systems with large time window show the result of a pile-up contaminated lifetime measurement and in particular the uniformly distributed random background when the super-singles filter is applied, see Figure 9 right.

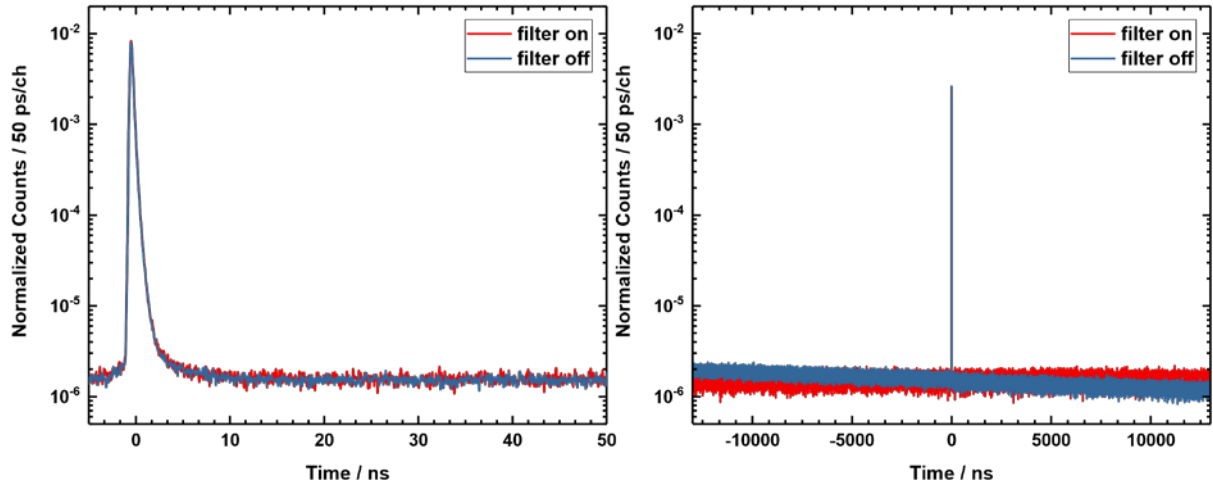


Figure 9: Normalized positron lifetime spectrum for a silicon reference material at a source-based setup with and without super-singles filter. Small time window (left) and large time window (right)

Inherently, the systematic bias appears negligible at narrow time intervals but the effect on the positron annihilation lifetime calculation cannot be neglected, since an adequate background calculation, either prior or after the main component of the spectrum, is essential. Consequently, taking this effect into account could prevent ghost components, incorrect lifetimes or false intensities.

## 2.6. Automated energy calibration

An underestimated source of error in PALS measurements are wrong or fluctuating energy windows. Here, the range in which a signal is grouped as a start or stop should be adequately adjusted. Changes of the detector gain within a measurement (unstable bias supply voltages, changing count rates, temperature variations) lead to improperly selected energy windows and possible systematic errors. Especially, changing detector count rates cause shifts in the signal amplitudes as shown in Figure 10.

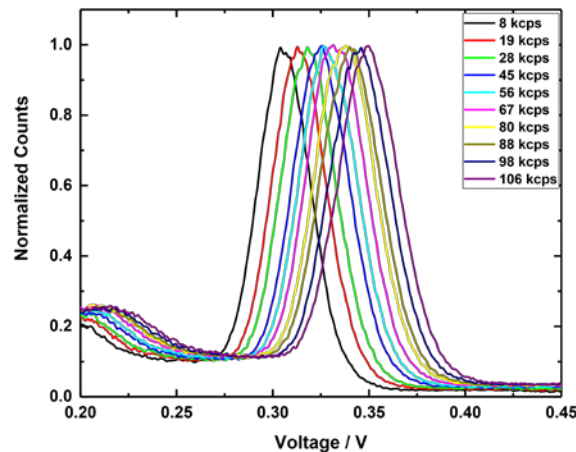


Figure 10: Pulse height spectra of the 511 keV annihilation radiation for different count rates.

Such linearity errors predominantly result from changing voltages when the electrode voltage is supplied from a resistive divider. The current given by the electrons at the last dynodes is no more negligible with

respect to the current through the voltage divider. The disturbance of the voltage distribution throughout the divider results in an increased gain with increasing count rate [38]. As a consequence, problems arise when the mostly voltage-defined windows of the pulse assignment at PALS experiments are set to fixed values, like analogue setups, while the count rate varies due to changes in the solid angle, beam steering or sample charging. In worst case, this leads to an almost complete shift of the annihilation peak out of the defined limits.

To realign the focus, a dynamic window determination was implemented. This no longer sets the window limits based on the voltage, instead performs a simplified energy calibration prior to each new measurement, allowing defined energy windows, see Figure 11 right.

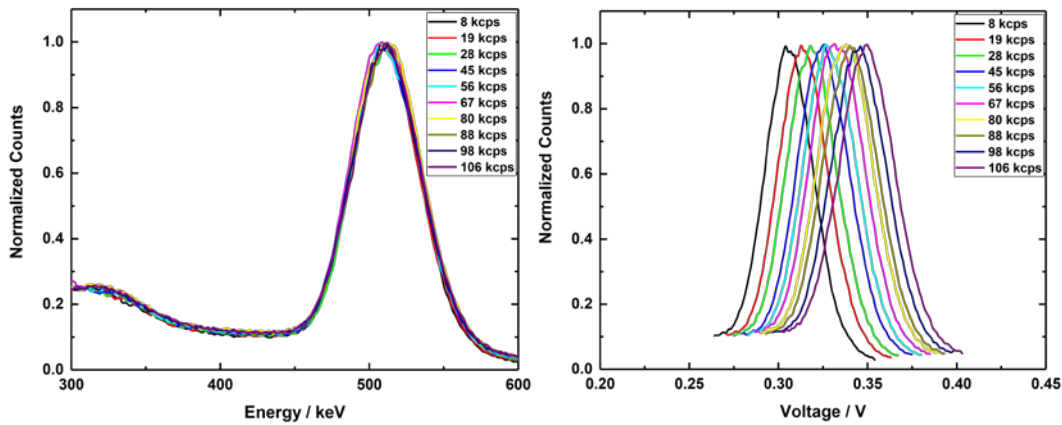


Figure 11: Shifted Pulse height spectrum into annihilation peak (left) dynamic window adjustment (right).

### 3. Summary

We demonstrate, how an efficient online data reduction, a numerically effective algorithm for pulse parameterization and utilization of multi-core parallelization led to a significantly improved data processing for positron annihilation lifetime spectroscopy. The approach constitutes the MePS setup as one of the first fully digital measurement systems considering beam-based positron annihilation lifetime spectroscopy facilities. The advantages include variable timing windows, arbitrarily selectable channel dispersions, acquisition times of less than 60 seconds per spectrum with  $10^7$  events each, absence of systematic bias due to pile-up events or energy window fluctuations, and, in addition, processing rates of up to 5.6 Mcps per channel for dynamic defect evolution studies. The presented system can be applied in future readily in neutron time -of-flight measurements [39], time-of-flight mass spectrometry or prompt gamma-ray timing in proton therapy [37] and been instrumental in the past in a variety of measurements ranging from materials for hard coatings [40], new vistas of the influence of atomic defects in voltage-driven magneto-ionics [41]–[43], material damages in heavily irradiated reactor materials [44] to superconductors for particle accelerators [45] and defect-related magnetism in FeAl alloys [46].

#### 4. References

- [1] R. Krause-Rehberg and H. S. Leipner, *Positron Annihilation in Semiconductors: Defect Studies*. Springer Berlin Heidelberg, 1999.
- [2] D. W. Gidley, W. E. Frieze, T. L. Dull, A. F. Yee, E. T. Ryan, and H.-M. Ho, "Positronium annihilation in mesoporous thin films," *Phys. Rev. B*, vol. 60, no. 8, pp. R5157–R5160, Aug. 1999, doi: 10.1103/PhysRevB.60.R5157.
- [3] A. Perkins and J. P. Carbotte, "Effect of the Positron-Phonon Interaction on Positron Motion," *Phys. Rev. B*, vol. 1, no. 1, pp. 101–107, Jan. 1970, doi: 10.1103/PhysRevB.1.101.
- [4] M. J. Puska and R. M. Nieminen, "Theory of positrons in solids and on solid surfaces," *Rev. Mod. Phys.*, vol. 66, no. 3, pp. 841–897, Jul. 1994, doi: 10.1103/RevModPhys.66.841.
- [5] O. E. Mogensen, *Positron Annihilation in Chemistry*, vol. 58. Berlin, Heidelberg: Springer Berlin Heidelberg, 1995.
- [6] A. Ore and J. L. Powell, "Three-Photon Annihilation of an Electron-Positron Pair," *Phys. Rev.*, vol. 75, no. 11, pp. 1696–1699, Jun. 1949, doi: 10.1103/PhysRev.75.1696.
- [7] C. Hugenschmidt, K. Schreckenbach, M. Stadlbauer, and B. Straßer, "First positron experiments at NEPOMUC," *Appl. Surf. Sci.*, vol. 252, no. 9, pp. 3098–3105, Feb. 2006, doi: 10.1016/j.apsusc.2005.08.108.
- [8] C. Hugenschmidt, C. Piochacz, M. Reiner, and K. Schreckenbach, "The NEPOMUC upgrade and advanced positron beam experiments," *New J. Phys.*, vol. 14, no. 5, p. 055027, May 2012, doi: 10.1088/1367-2630/14/5/055027.
- [9] A. van Veen *et al.*, "Intense Positron Sources and their Applications," *Mater. Sci. Forum*, vol. 363–365, pp. 415–419, Apr. 2001, doi: 10.4028/www.scientific.net/MSF.363-365.415.
- [10] O. Doron, S. R. Biegalski, S. O'Kelly, and B. J. Hurst, "Development of a transport system for the copper source of the Texas Intense Positron Source facility," *Nucl. Instruments Methods Phys. Res. Sect. B Beam Interact. with Mater. Atoms*, vol. 243, no. 1, pp. 247–249, Jan. 2006, doi: 10.1016/j.nimb.2005.07.204.
- [11] J. Moxom, A. G. Hathaway, and A. I. Hawari, "Out of core testing of the North Carolina State University PULSTAR reactor positron beam," in *2007 IEEE Nuclear Science Symposium Conference Record*, 2007, pp. 2343–2348, doi: 10.1109/NSSMIC.2007.4436615.

- [12] A. Yabuuchi *et al.*, "Evaluation of a positron-beam-pulsing system in KUR reactor-based positron beam facility," *J. Phys. Conf. Ser.*, vol. 791, no. 1, p. 012013, Jan. 2017, doi: 10.1088/1742-6596/791/1/012013.
- [13] R. H. Howell, M. J. Fluss, I. J. Rosenberg, and P. Meyer, "Low-energy, high-intensity positron beam experiments with a linac," *Nucl. Instruments Methods Phys. Res. Sect. B Beam Interact. with Mater. Atoms*, vol. 10–11, pp. 373–377, May 1985, doi: 10.1016/0168-583X(85)90272-1.
- [14] N. Oshima *et al.*, "Development of Positron Microbeam in AIST," *Mater. Sci. Forum*, vol. 607, pp. 238–242, Nov. 2008, doi: 10.4028/www.scientific.net/MSF.607.238.
- [15] K. Wada *et al.*, "New experiment stations at KEK Slow Positron Facility," *J. Phys. Conf. Ser.*, vol. 443, no. 1, p. 012082, Jun. 2013, doi: 10.1088/1742-6596/443/1/012082.
- [16] M. Jungmann *et al.*, "First Experiments with MePS," *J. Phys. Conf. Ser.*, vol. 443, no. 1, p. 012088, Jun. 2013, doi: 10.1088/1742-6596/443/1/012088.
- [17] H. Saito, Y. Nagashima, T. Kurihara, and T. Hyodo, "A new positron lifetime spectrometer using a fast digital oscilloscope and BaF<sub>2</sub> scintillators," *Nucl. Instruments Methods Phys. Res. Sect. A Accel. Spectrometers, Detect. Assoc. Equip.*, vol. 487, no. 3, pp. 612–617, Jul. 2002, doi: 10.1016/S0168-9002(01)02172-6.
- [18] H. Saito and T. Hyodo, "Improvement in the gamma-ray timing measurements using a fast digital oscilloscope," *Radiat. Phys. Chem.*, vol. 68, no. 3–4, pp. 431–434, Oct. 2003, doi: 10.1016/S0969-806X(03)00199-3.
- [19] K. Rytsölä, J. Nissilä, J. Kokkonen, A. Laakso, R. Aavikko, and K. Saarinen, "Digital measurement of positron lifetime," *Appl. Surf. Sci.*, vol. 194, no. 1–4, pp. 260–263, Jun. 2002, doi: 10.1016/S0169-4332(02)00128-9.
- [20] J. Nissilä, K. Rytsölä, R. Aavikko, A. Laakso, K. Saarinen, and P. Hautojärvi, "Performance analysis of a digital positron lifetime spectrometer," *Nucl. Instruments Methods Phys. Res. Sect. A Accel. Spectrometers, Detect. Assoc. Equip.*, vol. 538, no. 1–3, pp. 778–789, Feb. 2005, doi: 10.1016/j.nima.2004.08.102.
- [21] F. Bečvář, J. Čížek, I. Procházka, and J. Janotová, "The asset of ultra-fast digitizers for positron-lifetime spectroscopy," *Nucl. Instruments Methods Phys. Res. Sect. A Accel. Spectrometers, Detect. Assoc. Equip.*, vol. 539, no. 1–2, pp. 372–385, Feb. 2005, doi: 10.1016/j.nima.2004.09.031.



- [22] M. Jardin, M. Lambrecht, A. Rempel, Y. Nagai, E. van Walle, and A. Almazouzi, "Digital positron lifetime spectrometer for measurements of radioactive materials," *Nucl. Instruments Methods Phys. Res. Sect. A Accel. Spectrometers, Detect. Assoc. Equip.*, vol. 568, no. 2, pp. 716–722, Dec. 2006, doi: 10.1016/j.nima.2006.08.087.
- [23] A. M. Krille, R. Krause-Rehberg, M. Jungmann, F. Bečvář, and G. Brauer, "Digital positron lifetime spectroscopy at EPOS," *Appl. Surf. Sci.*, vol. 255, no. 1, pp. 93–95, Oct. 2008, doi: 10.1016/j.apsusc.2008.05.215.
- [24] L. Hui, S. Yundong, Z. Kai, P. Jingbiao, and W. Zhu, "A simplified digital positron lifetime spectrometer based on a fast digital oscilloscope," *Nucl. Instruments Methods Phys. Res. Sect. A Accel. Spectrometers, Detect. Assoc. Equip.*, vol. 625, no. 1, pp. 29–34, Jan. 2011, doi: 10.1016/j.nima.2010.10.005.
- [25] R. Ye *et al.*, "Coincidence time resolution investigation of BaF<sub>2</sub>-based H6610 detectors for a digital positron annihilation lifetime spectrometer," *J. Instrum.*, vol. 15, no. 6, Jun. 2020, doi: 10.1088/1748-0221/15/06/P06001.
- [26] J. J. Ge, Z. W. Xue, L. H. Cong, and H. Liang, "Development of a TDC-based digital positron annihilation lifetime spectrometer," *J. Instrum.*, vol. 15, no. 3, Mar. 2020, doi: 10.1088/1748-0221/15/03/P03034.
- [27] F. Bečvář, J. Čížek, and I. Procházka, "High-resolution positron lifetime measurement using ultra fast digitizers Acqiris DC211," *Appl. Surf. Sci.*, vol. 255, no. 1, pp. 111–114, Oct. 2008, doi: 10.1016/j.apsusc.2008.05.184.
- [28] F. Bečvář, "Methodology of positron lifetime spectroscopy: Present status and perspectives," *Nucl. Instruments Methods Phys. Res. Sect. B Beam Interact. with Mater. Atoms*, vol. 261, no. 1–2, pp. 871–874, Aug. 2007, doi: 10.1016/j.nimb.2007.03.042.
- [29] R. Aavikko, K. Rytsölä, J. Nissilä, and K. Saarinen, "Stability and Performance Characteristics of a Digital Positron Lifetime Spectrometer," *Acta Phys. Pol. A*, vol. 107, no. 4, pp. 592–597, Apr. 2005, doi: 10.12693/APhysPolA.107.592.
- [30] M. Nakhostin, *Signal Processing for Radiation Detectors*. Hoboken: John Wiley & Sons, Inc, 2018.
- [31] F. Gabriel *et al.*, "The Rossendorf radiation source ELBE and its FEL projects," *Nucl. Instruments Methods Phys. Res. Sect. B Beam Interact. with Mater. Atoms*, vol. 161–163, pp. 1143–1147, Mar. 2000, doi: 10.1016/S0168-583X(99)00909-X.
- [32] A. Wagner, M. Butterling, M. O. Liedke, K. Potzger, and R. Krause-Rehberg, "Positron annihilation lifetime and Doppler broadening spectroscopy at the ELBE facility," in *AIP Conference Proceedings*, 2018, vol. 1970, p. 040003, doi: 10.1063/1.5040215.

- 425 [33] B. Y. Tong, "Negative Work Function of Thermal Positrons in Metals," *Phys. Rev. B*, vol.  
426 5, no. 4, pp. 1436–1439, Feb. 1972, doi: 10.1103/PhysRevB.5.1436.
- 427 [34] E. Hirschmann, "Analyse der Porenstruktur in Schichtsystemen von kontrolliert  
428 extrahierten Natrium-Borosilikat-Glasplatten am digital optimierten monoenergetischen  
429 Positronen-Strahl des HZDR," Martin-Luther-Universität Halle-Wittenberg, 2021.
- 430 [35] D. A. Gedcke and W. J. McDonald, "A constant fraction of pulse height trigger for  
431 optimum time resolution," *Nucl. Instruments Methods*, vol. 55, pp. 377–380, Jan. 1967,  
432 doi: 10.1016/0029-554X(67)90145-0.
- 433 [36] A. S. Householder, *Principles of Numerical Analysis*. McGraw-Hill Book Company, Inc.,  
434 New York, 1953.
- 435 [37] C. Golnik *et al.*, "Range assessment in particle therapy based on prompt  $\gamma$ -ray timing  
436 measurements," *Phys. Med. Biol.*, vol. 59, no. 18, pp. 5399–5422, Sep. 2014, doi:  
437 10.1088/0031-9155/59/18/5399.
- 438 [38] S.-O. Flyckt and C. Marmonier, *PHOTOMULTIPLIER TUBES principles & applications*.  
439 Brive: Photonis, 2002.
- 440 [39] J. Klug *et al.*, "Development of a neutron time-of-flight source at the ELBE accelerator,"  
441 *Nucl. Instruments Methods Phys. Res. Sect. A Accel. Spectrometers, Detect. Assoc.*  
442 *Equip.*, vol. 577, no. 3, pp. 641–653, Jul. 2007, doi: 10.1016/j.nima.2007.04.132.
- 443 [40] P. Gasparotto *et al.*, "Mapping the Structure of Oxygen-Doped Wurtzite Aluminum  
444 Nitride Coatings from Ab Initio Random Structure Search and Experiments," *ACS Appl.*  
445 *Mater. Interfaces*, vol. 13, no. 4, pp. 5762–5771, Feb. 2021, doi:  
446 10.1021/acsami.0c19270.
- 447 [41] J. de Rojas *et al.*, "Voltage-driven motion of nitrogen ions: a new paradigm for magneto-  
448 ionics," *Nat. Commun.*, vol. 11, no. 1, p. 5871, Dec. 2020, doi: 10.1038/s41467-020-  
449 19758-x.
- 450 [42] J. Rojas *et al.*, "Boosting Room-Temperature Magneto-Ionics in a Non-Magnetic Oxide  
451 Semiconductor," *Adv. Funct. Mater.*, vol. 30, no. 36, p. 2003704, Sep. 2020, doi:  
452 10.1002/adfm.202003704.
- 453 [43] A. Quintana *et al.*, "Voltage-Controlled ON–OFF Ferromagnetism at Room Temperature  
454 in a Single Metal Oxide Film," *ACS Nano*, vol. 12, no. 10, pp. 10291–10300, Oct. 2018,  
455 doi: 10.1021/acsnano.8b05407.
- 456 [44] S. Agarwal *et al.*, "A new mechanism for void-cascade interaction from nondestructive  
457 depth-resolved atomic-scale measurements of ion irradiation–induced defects in Fe,"  
458 *Sci. Adv.*, vol. 6, no. 31, p. eaba8437, Jul. 2020, doi: 10.1126/sciadv.aba8437.

- 459 [45] M. Wenskat *et al.*, “Vacancy-Hydrogen Interaction in Niobium during Low-Temperature  
460 Baking,” *Sci. Rep.*, vol. 10, no. 1, p. 8300, Dec. 2020, doi: 10.1038/s41598-020-65083-  
461 0.
- 462 [46] J. Ehrler *et al.*, “The role of open-volume defects in the annihilation of antisites in a B2-  
463 ordered alloy,” *Acta Mater.*, vol. 176, pp. 167–176, Sep. 2019, doi:  
464 10.1016/j.actamat.2019.06.037.
- 465